Fasciola gigantica: ultrastructural cytochemistry of the tegumental surface in newly-excysted metacercariae and *in vitro*-penetrated juvenile flukes informs a concept of parasite defence at the interface with the host.

R.E.B. Hanna[a*], D. Moffett[a], M. W. Robinson[b], W.G.Z.O. Jura[c], G.P. Brennan[b], I. Fairweather[b], L.T. Threadgold[b]

[a] Veterinary Sciences Division, Agri-Food and Biosciences Institute (AFBI), Stormont, Belfast BT4 3SD, United Kingdom

[b] School of Biological Sciences, The Queen's University of Belfast, Belfast BT9 5DL, United Kingdom

[c] Department of Zoology, Maseno University, Maseno, Kenya

[*]corresponding author:

e-mail: bob.hanna@afbini.gov.uk

telephone +44(0)2890525615

Abstract

Cytochemical staining techniques were carried out *en bloc* with *in vitro* excysted and gut-penetrated *Fasciola gigantica* larvae in order to visualise the glycocalyx of the tegument, a structure which comprises the parasite component of the host-parasite interface, yet is incompletely preserved by conventional fixation and preparation

techniques for electron microscopy. Positive reactivity with ruthenium red and periodic acid-thiocarbohydrazine-osmium (PATCO) techniques revealed that the glycocalyx is polyanionic and carbohydrate-rich throughout its depth. It comprises a trilaminate arrangement, with a thin dense zone and fibrillar layer closely apposed to the outer aspect of the apical plasma membrane, invested by an irregular thick mucopolysaccharide capsule. The latter, not recorded in adult flukes, may represent a specific adaptation to facilitate invasion in the face of host immunity, and may also protect the parasite surface from the action of host- and parasite-derived proteases. Early in the invasion of a naïve host, the glycocalyx may be partly responsible for triggering the responses of innate immunity, while later in infection, or when an anamnestic response is initiated in an immunocompetent host, the antibodies and activated lymphocytes of specific acquired immunity are invoked to interact with the parasite surface. The cytochemical properties of the glycocalyx, together with its potential for dynamic turnover due to exocytosis of the T0 tegumental secretory bodies, are likely to aid neutralisation of potentially damaging immune effectors and ensure their removal from the vicinity of the parasite by sloughing in complex with glycocalyx components.

Key words: *Fasciola gigantica; in vitro* excystment and gut-penetration; tegumental ultrastructure and cytochemistry; glycocalyx; parasite defence; innate and acquired immunity.

1. Introduction

While infection by *Fasciola gigantica* is considered to represent a significant constraint on the productivity of domestic ruminants throughout Asia and Africa, impacting on global food production as the demand for meat production increases in developing countries, relatively few studies have addressed the structural and molecular adaptations that enable this parasite to successfully invade a wide range of host species, including humans (Spithill et al., 1999a; Piedrafita et al., 2010). The topography and ultrastructure of the tegument of bile-duct inhabiting adult *F. gigantica* were examined by Ahmad et al. (1988), Sobhon et al. (1998) and Dangprasert et al. (2001). The carbohydrate-rich negatively charged glycocalyx that coats the outer aspect of the tegument may help the parasite to evade the antibody-dependant cell-mediated cytotoxicity (ADCC) reaction of the host, and surface derived antigens can elicit strong immunological responses from the host (Sobhon et al., 1998). Recently, an examination of the ultrastructure of the surface in the invading larvae of *F. gigantica* verified the cytological origins of the glycocalyx of the tegument, and highlighted its potential for dynamic renewal at the interface with the host (Hanna et al., 2019). In newly-excysted *F. gigantica,* the tegumental perikarya ('tegumental cells'), which lie beneath the surface syncytium of the tegument, but are connected to it by cytoplasmic tubules passing between the interposing muscle blocks, are packed with T0 secretory bodies. These T0 bodies rapidly migrate into the surface syncytium and discharge their contents at the apical plasma membrane to maintain the surface glycocalyx during penetration of the larvae through the gut wall of the host (Hanna et al., 2019). In *Fasciola* spp., the glycocalyx, which completely envelops the surface of the invading larva and represents the parasite component of the host-parasite interface, is actively sloughed and rapidly replaced to protect the larva from immune-mediated attack by the host (Hanna, 1980a;

Fairweather et al., 1999; Hanna et al., 2019). However, early in the invasion of a naïve host animal, the larval flukes are unlikely to encounter the effectors of acquired immunity (cell-mediated or humoral), since penetration of the intestine wall and migration to the liver capsule is relatively rapid (Andrews, 1999). Instead, recognition of tissue damage and the presence of parasite surface components is likely to initiate acute inflammation, so the surface of the invading fluke larvae will initially come under attack from effectors such as major basic protein (MBP) from eosinophils and natural killer cells, before ultimately encountering the humoral and cell-mediated components of acquired immunity (Dalton et al., 2013). In these interactions, the glycocalyx embodies the first line of parasite defence at the interface with the host, and knowledge of its structure and chemical constitution is fundamental to our understanding of the ability of *Fasciola* spp. to survive and successfully invade immunologically primed as well as naïve hosts. With conventional fixation for electron microscopy, only a fraction of the thickness of the glycocalyx in adult *F. hepatica* is preserved, and an array of cytochemical tests is necessary to reveal its fine structure (Threadgold, 1976). The aim of the present study was to visualise the glycocalyx in those stages of *F. gigantica* that are first exposed to the innate and/or adaptive effectors of immunity in the host, with a view to informing our understanding of the early mechanisms of defence in this highly successful parasite.

2. Methods and materials

2.1 General

The preparative stages of this study, namely collection, excystment, penetration, *en bloc* cytochemical reactions, fixation and resin embedding of *F. gigantica* larvae for

electron microscopy were carried out in the (then) East African Veterinary Research Organisation, Muguga, Kenya, in 1975. Resin blocks were stored dry in sealed plastic containers at 20ºC. The quality of fixation and resin infiltration of the various batches of larvae was checked by sectioning representative resin blocks 1-2 years after the incubations were carried out. Comprehensive sectioning and examination of the material was carried out at the Veterinary Sciences Division, Agri-Food and Biosciences Institute, Belfast, in 2019. No change or deterioration was detected in the preservation or sectioning quality of the embedded larvae from the time of the initial test sectioning 42 years earlier.

Full details of the source of material, techniques used for *in vitro* excystment and gut-penetration of *F.gigantica* larvae, and basic preparative methods for electron microscopy were reported recently (Hanna et al., 2019). Briefly, metacercarial cysts from laboratory-maintained *Lymnaea natalensis* that had been infected with miracidia of *F. gigantica*, were hatched using an excystment protocol (based on the method of Dixon, 1964, for *F. hepatica*) that provided CO_2 and bile components, under reducing conditions, at 37ºC. Newly-excysted larvae, suspended in Eagle's MEM medium with antibiotics, were pipetted into a bag of mouse jejunum which was tied off at each end with cotton thread. The larvae were allowed to penetrate through the gut wall into fresh Eagle's medium, over a period of 5 h.

2.2 Conventional fixation

Some newly-excysted and some penetrated larvae were fixed for 5h at 4ºC with 4% (w/v) Millonig phosphate-buffered glutaraldehyde (pH 7.3) containing 3% (w/v) sucrose, buffer-washed, osmicated, dehydrated through alcohol and propylene oxide, infiltrated and embedded in Araldite resin (then supplied by Ciba-Geigy; currently supplied by Agar Scientific Ltd., Essex, UK). Further batches of larvae were

fixed with 3% (w/v) glutaraldehyde in 0.2 M cacodylate buffer (pH 7.2) for 5h at 4ºC and rinsed in 0.2 M cacodylate buffer prior to osmication, dehydration and embedding in Araldite resin. The buffers used in the preparation of these batches of larvae were the same as those used in the respective cytochemical reactions detailed below. Batches of newly-excysted and of penetrated larvae were treated *en bloc* for cytochemical investigations, as follows.

2.3 Ruthenium red technique

Newly-excysted and penetrated larvae were separately fixed with 3% (w/v) glutaraldehyde in 0.2 M cacodylate buffer, pH 7.2, containing 8.0 mM ruthenium red (then supplied by Sigma Chemicals Co., St. Louis, MO, USA) for 5h at 4ºC. The larvae were then rinsed in 0.2 M cacodylate buffer, pH 7.2, containing 8.0 mM ruthenium red for 10 min, and post-fixed with 1% (w/v) osmic acid in cacodylate buffer for 1h prior to dehydration and embedding in Araldite embedding resin. Neuraminidase control material was fixed with 3% (w/v) glutaraldehyde in 0.2 M cacodylate buffer for 3h, rinsed in 0.2 M cacodylate buffer, and then incubated in neuraminidase (30 units in 0.1 M acetate buffer, pH 5.5; then supplied by Sigma Chemicals Co., St. Louis, MO, USA) for 1 h at 37ºC. These larvae were then fixed for a further period of 5h with 3% (w/v) glutaraldehyde in 0.2 M cacodylate buffer containing 8.0 mM ruthenium red, and rinsed with 0.2 M cacodylate buffer containing 8.0 mM ruthenium red, prior to osmication, dehydration and embedding (Rambourg, 1971; Threadgold, 1976; Pearse, 1985).

2.4 Periodic acid-thiocarbohydrazine-osmium (PATCO) technique

Newly-excysted and penetrated larvae were fixed overnight at room temperature in 4% (w/v) paraformaldehyde in Millonig buffer (pH 7.3) containing 1% (w/v) NaCl and 0.5 mM $CaCl_2$. They were then treated for a further 2h in 4% Millonig-buffered

paraformaldehyde with NaCl and $CaCl_2$ containing 1% (w/v) periodic acid, and subsequently washed for 4h with Millonig buffer alone. The larvae were then immersed in a solution of 1% (w/v) thiocarbohydrazine (TCH) in 25% (w/v) acetic acid for 48h at room temperature. Following a 30 min rinse in water, the larvae were exposed to osmic acid vapour in a sealed wet chamber for 3h at 40ºC, washed again with distilled water for 1h, and finally dehydrated and embedded in Araldite. Control batches of larvae were prepared by (a) omitting the periodic acid treatment; (b) treating fixed larvae, before or after periodate exposure, with 0.3% (w/v) aniline in 0.5% (w/v) acetic acid for 2h or with 1% (w/v) aqueous dimedone for 24h to block pre-existing or generated aldehyde groups; (c) treating fixed larvae with neuraminidase (30 units in 0.1 M acetate buffer, pH 5.5) for 1 h at 37ºC, before exposure to periodic acid. All control larvae were then treated with TCH and osmic acid vapour, washed, dehydrated and embedded as described above (Rambourg, 1971; Threadgold, 1976; Pearse, 1985)

2.5 Electron microscopy

Ultrathin sections (100-120 nm thick) were cut from the Araldite resin blocks using a Leica EM UC7 ultramicrotome, mounted on uncoated nickel grids, double stained with uranyl acetate and lead citrate or left unstained, and viewed in a JEOL JEM-1400 transmission electron microscope with an AMT Activue XR16 digital camera system, operating at an accelerating voltage of 80 kV. Generally, images were saved at an instrument magnification of X25,000, and measurements of selected ultrastructural features were carried out using at least 100 replicates of each feature, accumulated from multiple images.

The cytochemical staining techniques employed, their respective controls and the purposes for which they were used are listed in Table 1.

3. Results

3.1 Ruthenium red technique

Ten *in vitro* gut-penetrated larvae of *F.gigantica* and ten newly-excysted larvae that had been treated *en bloc* with ruthenium red were examined and the sections were compared with equivalent sections of conventionally-fixed larvae, and with sections of larvae that had been treated with neuraminidase before ruthenium red treatment. The appearance of all ten larvae within each of the two groups (penetrated and newly-excysted respectively) corresponded closely, as did the larvae within each of the control groups. The penetrated larvae treated with ruthenium red all show a continuous line of dense staining 14.6 ± 4.3 nm thick, on the outer aspect of the apical plasma membrane of the tegumental syncytium, following it closely along all the invaginations and prominences of the surface (Fig. 1a and b). Immediately beneath the dense line, the pale-staining central core of the trilaminar apical membrane can usually be resolved, and the inner dense zone of the membrane is also usually apparent (Fig. 1a and b). In most regions, the superficial aspect of this surface zone features a rather sparse fibrillar layer (32.2 ± 8.1 nm thick, including the underlying dense line, Fig. 1a), or is covered with lightly-stained, relatively featureless ‘hyaline’ material (so-called because of its relatively low electron density, generally homogenous appearance and lack of cellular or fibrous structure, in comparison to the dense line and fibrillar layers). The latter forms a discontinuous outer layer, missing in some areas and, where present, very variable in thickness (98.7 ± 67.2nm, Fig. 1b). It sometimes appears as globules on the surface (Fig. 1c), and may sometimes incorporate electron-dense patches or fibrous material, resembling components of the fibrillar layer (Fig. 1c). The dense line, intimately

196 associated with the outer aspect of the surface membrane, is stained most
197 prominently in those areas where the hyaline layer is lacking. In regions where it is
198 covered by the hyaline layer, staining is less pronounced, although usually the
199 course of the dense line can be traced beneath the hyaline layer (Fig. 1 b and c). In
200 some areas the hyaline material seems to envelop the underlying dense line and
201 fibrillar layer (Fig. 1c), whereas in other areas it is seen partially elevating the dense
202 line and fibrillar layer (Fig. 1d). Occasionally the entire ruthenium-stained complex,
203 including dense line, fibrillar material and/or hyaline material is seen sloughing from
204 the surface in the form of membranous strips, whorls or vesicles (Fig. 1e). In the
205 newly-excysted larvae that had not been allowed to penetrate through mouse gut
206 tissue, the dense line and fibrillar layer on the superficial aspect of the apical plasma
207 membrane, stained by ruthenium red, are also apparent. In these larvae the area
208 occupied by the hyaline material appears rather less than in the penetrated larvae,
209 and its distribution is more irregular (Fig. 2a). In neither the newly-excysted larvae
210 nor the penetrated larvae does the ruthenium red-stained zone extend into the
211 superficial cytoplasm of the tegumental syncytium, although the lining of small
212 invaginations and valleys that have open contact with the surface exhibit staining
213 (Fig. 1b and 2a). Beneath the surface of the syncytium, the cytoplasm and structures
214 such as T0 secretory bodies, mitochondria, invaginations of the basal plasma
215 membrane and spines are not stained by ruthenium red. The T0 bodies, which are
216 membrane-bound, often ellipsoidal in shape (143.1 ± 23.2 nm X 80.8 ± 13.9 nm) and
217 of moderate electron density, are often seen close beneath the apical plasma
218 membrane, apparently discharging their content into the hyaline layer or immediately
219 below the dense layer (Fig. 2b and c). In so-doing they assume a flattened or rod-like

220 shape (146.5 ± 27.7 nm), remaining within the apical cytoplasm of the syncytium
221 (Fig. 2 c).

222 3.2 Controls for ruthenium red technique

223 In conventionally-fixed larvae (where ruthenium red treatment was omitted and
224 fixation was carried out using either cacodylate-buffered or Millonig phosphate-
225 buffered glutaraldehyde), the apical plasma membrane of the tegumental syncytium
226 is less well-defined and features an apparently discontinuous and 'fuzzy' outer zone,
227 that is less dense and thinner (7.1 ± 2.1 nm) than the outer zone in the ruthenium
228 red-treated larvae. Superficial filaments and hyaline patches are lacking from this
229 control material (Fig. 2d). In neuraminidase-treated control larvae fixed with
230 ruthenium red present, the dense line of staining that characterises the larvae in the
231 test groups is present but thinner (9.9 ± 3.0 nm) and less well-defined than in the
232 test material, with only occasional patches of fibrillar or hyaline material on the
233 surface (Fig. 2e).

234 3.3 PATCO technique

235 The batches of penetrated and newly-excysted larvae that were treated *en bloc*
236 using the PATCO reaction, together with the relevant control batches, were fixed
237 with buffered paraformaldehyde rather than glutaraldehyde and as a result the
238 ultrastructural preservation is poor. In addition, the prolonged exposure to osmic acid
239 vapour, necessary to achieve satisfactory visualisation of the glycocalyx, tended to
240 result in cracking and breaking of the surface (Fig. 3a and b). Sections were
241 examined in the electron microscope, usually without the use of conventional double
242 staining (uranyl acetate followed by lead citrate). While the latter would have
243 improved resolution, it might have interfered with the interpretation of the *en bloc*

staining. The results for all ten larvae within each of the two experimental groups (penetrated and newly-excysted respectively) corresponded, as did those for the larvae within the control groups. The surface of the apical tegumental membrane in each of the PATCO-treated penetrated larvae features a superficial zone of dense staining that varies considerably in thickness in different regions of the body (96.4 ± 47.1 nm; range approximately 40 – 180 nm), but without a recognisable anatomical distribution (Fig. 3a and b). The attachment of this zone, while following closely the contours of the surface (Fig. 3a) appears tenuous in places, with a narrow clear space sometimes evident between the dense material and the underlying apical surface (Fig. 3b). In some areas the dense zone appears fragmented, detaching and apparently sloughing from the surface (Fig. 3c). In the apical cytoplasm of the syncytium the T0 bodies show positive staining, which is often more dense in those T0 bodies close to the surface (Fig. 3a). Occasionally T0 bodies are seen to be in contact with the surface, apparently discharging their content into the dense zone (Fig. 3d). Elsewhere, there is scattered dense staining over the cytoplasm (Fig. 3a), but it is not clearly associated with T0 bodies, although spine protein, mitochondria and the dense bodies previously described as tertiary lysosomes or heterophagosomes (Hanna et al., 2019) are generally unstained or only lightly stained (Fig. 3c and d). Newly-excysted larvae that had not penetrated through mouse gut displayed a similar staining pattern to the penetrated larvae, in that a thick zone of dense staining (105.7 ± 40.6 nm; range approximately 50 – 200 nm) is present over a large proportion of the apical plasma membrane (Fig. 3e), although in many places this zone appears to be fragmented and detaching. T0 bodies, close to the surface, are positively stained, and there is scattered positive staining over the cytoplasm.

3.4 Controls for PATCO technique

In control larvae (both penetrated and newly-excysted specimens), where periodic acid treatment was omitted, there is no dense zone of PATCO staining on the surface, although in some areas the apical plasma membrane appears to be delineated (Fig. 4a), and there is light speckled dense staining (corresponding to non-specific deposition of osmium dioxide) over the cytoplasm of the tegument. The T0 bodies are unstained. In those control larvae where a blocking step (using aniline or dimedone) was included before the periodic acid treatment, the surface of the tegument bears a dense but irregular zone of staining similar to that described above for the test larvae. However, in the larvae treated with aniline or dimedone after periodic acid treatment, but before the TCH step prior to osmication, the surface of the tegument is generally unstained, or bears irregular stained particles and fragments, corresponding to the trilaminar apical membrane (Fig. 4b and c). In these larvae the T0 bodies in the cytoplasm react positively. In the neuraminidase-treated control larvae, surface staining after the PATCO reaction is reduced, in comparison to the test larvae. The thick superficial zone of dense staining is generally lacking, represented only by dense fragments on the apical plasma membrane (Fig. 4d). As with the blocking controls and the test sections, there is scattered dense staining over the cytoplasm which is not associated with T0 bodies.

4. Discussion

4.1 General

In a study by Threadgold (1976) on the ultrastructure and histochemistry of the tegumental glycocalyx of adult *F. hepatica,* staining techniques, including ruthenium

red and PATCO, were carried out on ultrathin sections of conventionally-fixed, resin-embedded flukes and also on freshly fixed '*en bloc'* preparations of fluke material. It was found that conventional preparative techniques, followed by staining of ultrathin sections, enabled visualisation of only about half the total thickness of the glycocalyx, while the histochemical tests applied *en bloc* gave a more accurate morphological and histochemical picture. For this reason, *en bloc* histochemical staining was adopted for the present study on penetrated and newly-excysted *F. gigantica* larvae, where the available experimental material was limited and the specimens for processing were relatively small. However, a disadvantage of *en bloc* histochemical staining is that reagents with a large molecular size such as ruthenium red, aniline, dimedone and neuraminidase may be unable to penetrate into the depth of the specimens, especially considering that the larvae under examination are enveloped and sequestered by the intact apical plasma membrane of the tegument (Hanna et al., 2019). Therefore the findings from the histochemical tests, with their appropriate controls, are valid for the surface features only, in particular the glycocalyx, and can provide only limited and qualified information on subsurface structures.

4.2 Glycocalyx structure

Considering the likely significance of the glycocalyx in the establishment of fluke infection in the host, its molecular constitution has been the subject of a number of investigations since its existence was confirmed by Threadgold (1976). It is envisaged that the superficial aspect of the tegument is covered by layer of glycoprotein, closely applied to the outer layer of the trilaminate apical plasma membrane and, from this 'backbone', oligosaccharide side chains containing terminal sialic acid residues project outwards into the host-parasite interface. In

addition, the oligosaccharide side chains of gangliosides project outwards between the structural proteins of the glycoprotein backbone, with their sphingosine bases anchored beneath, in the electron-lucid lipid component of the plasma membrane (Fig. 5). Due partly to the terminal sialic acid residues in these oligosaccharide side chains, the glycocalyx is polyanionic throughout its thickness, and has a net negative charge, enabling it to be stained by cationic dyes such as ruthenium red, and, in addition, the carbohydrate-rich nature of the glycoproteins and gangliosides imparts reactivity with periodic acid-Schiff-type techniques such as PATCO (Threadgold, 1976). The essential features of this model of the glycocalyx in *F. hepatica* have been supported by subsequent studies that have utilised lectins to characterise the carbohydrate moieties of the glycocalyx, revealing the predominance of mannose, glucosamine or glucose moieties and *N*-glycosylated proteins (Rogan and Threadgold, 1984; Ravidà et al., 2016; de la Torre-Escudero et al., 2019). The significance of these surface glycoconjugates of *F. hepatica* in relation to the uptake of parasite-derived material by host cells, immune modulation and vaccine development were discussed by de la Torre-Escudero et al. (2011), Dalton et al. (2013) and Ravidà et al. (2016). Recently, it was observed that oligosaccharides present on the surface of extracellular vesicles (EVs) secreted by adult *F. hepatica* were resistant to *exo*- and *endo*-glycosidases that commonly modify mammalian structures (de la Torre-Escudero et al., 2019). Whilst having *N*-linked oligosaccharides that are resistant to degradation in the host microenvironment would be advantageous to the parasite, it remains to be determined whether the glycans displayed on the tegumental surface (which are distinct from those of EVs) show the same level of resistance.

4.3.Ruthenium red technique

343 *4.3.1 Ruthenium red test larvae*

344 The cationic dye, ruthenium red, acting in combination with osmium tetroxide
345 (Pearse, 1985), deposited a dense line of staining along the glycocalyx of the apical
346 trilaminate membrane of the tegument in both the penetrated and the newly-
347 excysted *F. gigantica* larvae, and a closely attached fibrillar layer of variable
348 thickness extended beyond the surface. This finding is consistent with that of
349 Threadgold (1976), who described a similar arrangement in adult *F. hepatica* stained
350 with ruthenium red. It also concurs with the observations of Sobhon et al. (1998) on
351 adult *F. gigantica*, that the surface of the tegument is coated with a negatively-
352 charged carbohydrate-rich glycocalyx layer and is the source of antigens that have
353 potential significance as candidate vaccines. In the larvae described here, the dense
354 line of the glycocalyx was of similar thickness to that recorded by Threadgold (1976)
355 (respectively 14.6 ± 4.3 nm for *F. gigantica* and 18.5 ± 6.5 nm for *F. hepatica*), but
356 the fibrillar layer was narrower, the total complex measuring 32.2 ± 8.1 nm thick
357 compared to 40.3 ± 15.6 nm for adult *F. hepatica.* Unlike the latter, the penetrated
358 larvae described here featured a hyaline layer of very variable thickness (98.7 ± 67.2
359 nm) over expanses of the apical tegumental surface, this layer being distributed
360 rather less consistently in the newly-excysted larvae than in the penetrated larvae.
361 This study on *F. gigantica* highlights, for the first time, the ultrastructural
362 cytochemistry of the tegumental glycocalyx in host-invading *Fasciola* larvae,
363 revealing it to be trilaminate, with both membrane-attached and labile components.
364 No comparable findings have been reported for *F. hepatica* larvae. The T0 bodies in
365 the tegumental syncytium were occasionally visualised in the process of discharging
366 their content into the surface layers, as was also noted by Hanna et al. (2019). It is
367 possible that the bounding membrane of the T0 bodies is lined internally by fixed

precursor components of the dense line and fibrillar layer, while the core contains labile mucopolysaccharides that contribute the unattached hyaline portion of the glycocalyx. On exocrine secretion of a T0 body, the membrane may sometimes be incorporated into the apical surface membrane, complete with attached glycocalyx, while it is proposed that the mucin-type T0 contents may flow over the surface to augment the labile chemico-physical protective barrier. On the other hand, after discharge of the labile component, the collapsed membrane of the T0 granule is often retained in the surface syncytium as a flattened sac, rather than contributing to the apical membrane (possibly reflecting molecular incompatibility between the apical membrane and the bounding membrane of T0 bodies). This may be a mechanism to prevent over-extension of the surface, and is possibly linked to active membrane recycling in the tegument (Hanna et al., 2019). As a labile component of the glycocalyx, the hyaline layer is likely to be readily removed during fixation, washing, staining, dehydration and embedding for electron microscopy, so its inconsistent appearance on the surface of larvae is not unexpected. In adult *F. hepatica,* studied by Threadgold (1976), there may be less need for a labile mucin-type protective layer because the bile duct environment is physico-chemically stable and relatively 'safe' from the effectors of innate and acquired immunity, compared to the gut wall and peritoneal environment experienced by the invading larvae (Hanna, 1980a). The T0 tegumental secretory bodies, characteristic of newly-excysted and invading *F. hepatica* and *F. gigantica,* are replaced by smaller dense T1 bodies in the liver-migrating juvenile flukes and adults (Bennett and Threadgold, 1975; Hanna et al., 2019) and, while these contain antigens in common with the T0 bodies (Hanna, 1980a, b), they may not contain precursors for an unattached mucin-type component of the glycocalyx. It was noted that ruthenium red staining does not

extend inward from the apical surface to the cytoplasm and organelles of the tegumental syncytium. This is because the large molecular size of the dye does not allow it to cross the undamaged plasma membrane of the *en bloc* preparations (Hayat, 1989).

4.3.2 Ruthenium red control larvae

Comparison of sections of conventionally-fixed larvae with sections of *en bloc* ruthenium red-treated larvae revealed that the glycocalyx is very much thinner in conventionally-treated material, lacking the fibrillar and hyaline layers which are fixed and visualised by the combination of ruthenium red and osmium tetroxide (Pearse,1985). The superficial aspect of the apical plasma membrane in the conventionally-fixed material exhibited only a 'fuzzy' layer, 7.1 ± 2.1 nm thick. Clearly, conventional fixation fails to preserve the glycocalyx of the larvae in its entirety, as was also noted by Threadgold (1976) for adult *F. hepatica*. Neuraminidase digestion of the *en bloc* preparations before fixation with ruthenium red present resulted in substantial reduction in staining of the fibrillar and hyaline layers of the glycocalyx, and partial loss of the dense layer. This is consistent with the presence of a significant sialic acid component in the glycocalyx, and is in accordance with the findings of Threadgold (1976) and Rogan and Threadgold (1984). On the other hand, the preliminary fixation and incubation steps carried out before ruthenium red treatment of these control larvae may, in themselves, have resulted in partial loss, particularly of the labile component of the glycocalyx, and resulted in enhanced exposure of the sialylated components to enzyme action. It is known that helminths, along with all invertebrates of the protostome lineage, lack the necessary enzymatic functionality to carry out sialylation of carbohydrate molecules (Varki and Schauer, 2009), so it is possible that sialic acid-bearing sugars in the

glycocalyx of *Fasciola* spp. could be host-derived, representing a mechanism of defence against the host's immune responses (Ravidà et al., 2016; McVeigh et al., 2018).

4.4 PATCO technique

4.4.1 PATCO test larvae

Fixation of larvae for *en bloc* PATCO staining was carried out with 4% (w/v) paraformaldehyde, rather than glutaraldehyde. Fixatives containing glutaraldehyde are avoided if tissues are to be stained by periodic acid Schiff (PAS)-related techniques because glutaraldehyde has two aldehyde groups per molecule, and tissues fixed in it will contain free aldehyde groups capable of undergoing Schiff-type reactions, resulting in non-specific background staining (Suvarna et al., 2018). Ultrastructural preservation is inferior, however, to that achievable with glutaraldehyde fixation. Thiocarbohydrazide, used here in the PATCO modification of the PAS technique to visualise the presence of carbohydrate in the oligosaccharide side chains of the glycocalyx, is a bidentate ligand which attaches to aldehyde groups released by periodic acid treatment and, at the other binding site, reacts with osmium tetroxide to deposit osmium dioxide at the site of staining (Hayat, 1989). Thus, the carbohydrate-rich surface components are fixed and rendered electron-dense by the PATCO reaction. With both the penetrated and the newly-excysted *F. gigantica* larvae, *en bloc* PATCO staining resulted in a thick zone of dense staining that was closely applied to the outer aspect of the apical plasma membrane of the tegument. While this zone is very variable in thickness, and frequently seen partially detached from the apical plasma membrane, at approximately 100 nm, it is significantly thicker than the equivalent zone described by Threadgold (1976) for PATCO-stained adult *F. hepatica* (26.0 ± 5.3 nm). However, like the surface zone in

adult *F. hepatica*, that in *F. gigantica* larvae was uniform in density throughout its thickness, without differentiation into dense line, fibrillar layer or hyaline layer, suggesting that all zones of the glycocalyx are carbohydrate-rich. This is consistent with the concept of a glycoprotein layer with oligosaccharide side chains and gangliosides, integral with the outer aspect of the surface membrane, but with an overlying labile or dynamic zone of mucopolysaccharide (also positive-staining by the PATCO technique), which is present in invading *F. gigantica* larvae, but lacking, or only weakly represented, in the adult worms. In the cytoplasm of the tegumental syncytium, the T0 bodies were stained by the PATCO reaction, consistent with glycoprotein and/or mucopolysaccharide content. Whilst other organelles in the syncytium, such as heterophagosomes, spines and mitochondria, were not stained by the PATCO technique, there was patchy dense staining over the cytoplasm itself. This may represent non-membrane-bound polymorphic masses of mucopolysaccharide that are associated with the basal infolds of the syncytium, and contribute to the osmoregulatory function of the tegument in *Fasciola* spp. (Threadgold and Brennan, 1978; Fairweather et al., 1999).

4.4.2 PATCO control larvae

As expected, control batches of larvae that were not exposed to periodic acid treatment gave negative results following TCH-osmium staining, confirming that the tissues did not contain indigenous or fixative-derived aldehyde groups, and that the reaction depended on periodate oxidation of 1-2 diol or α-hydroxyamino linkages in the oligosaccharide side chains (Pearse,1985). Aniline and dimedone treatment after periodic acid oxidation prevented staining, since these agents bind with the periodate-generated aldehyde groups, blocking subsequent reactivity with TCH-osmium. The results of the blocking tests are consistent with the carbohydrate-rich

nature of the glycoprotein and ganglioside side chains as well as that of the labile mucopolysaccharide envelope. Neuraminidase digestion substantially reduced staining of the glycocalyx on the surface of *en bloc* preparations but, like aniline and dimedone blockage, the effect did not penetrate below the apical plasma membrane, so reactivity in the cytoplasm of the surface syncytium, including that due to T0 bodies, was unaffected. Neuraminidase acts by cleaving sialic acid moieties, believed to terminate the oligosaccharide side chains of glycoproteins and glycosides in the dense line and fibrillar layer (Threadgold, 1976). While mucopolysaccharides of the hyaline layer have not been shown to contain sialic acid, it is possible that loss of this layer in the neuraminidase control material was facilitated by destabilisation of the underlying dense line and fibrillar layer, but the additional enzyme-incubation stage prior to periodic acid treatment may, in itself, have contributed to non-specific removal of the labile component of the glycocalyx.

4.5 Role of the glycocalyx in innate and acquired immunity

It is probable that the structural and histochemical features of the tegumental glycocalyx in *F. gigantica* larvae have evolved to confront and abrogate the effectors of innate and acquired immunity in the naïve and immunocompetent host. The complex polysaccharides comprising the side chains of glycoprotein and ganglioside molecules, together with epithelial cell damage mediated by gut wall penetration, will likely trigger receptors on tissue macrophages and dendritic cells (eg. toll-like receptors and damage-associated molecular pattern [DAMP] receptors) and activate the inflammasome and complement system. The resultant expression, by the host, of inflammatory mediators including chemokines will attract eosinophils to the area, with release of major basic protein (Jackson et al., 2009; Allen and Maizels, 2011; Dalton et al., 2013; Kumar et al., 2018). This highly cationic molecule, cytotoxic to

493 many parasites, is likely to bind with, and perhaps be inactivated by, the polyanionic
494 glycocalyx components. Furthermore, the thick, labile and replaceable glycocalyx
495 may help protect the parasite surface from host-gut-derived proteases and the
496 secreted proteases (typically cathepsins B and L) originating from the developing
497 gastrodermal epithelium of the parasite itself, and used to achieve penetration of the
498 host tissues (Bennett, 1975; Cwiklinski et al., 2019). Later in the invasion process, or
499 as a result of anamnestic response in an immunocompetent host, the parasite
500 surface will become the target for the effectors of acquired immunity. Components of
501 the tegumental glycocalyx in *F. hepatica* engender the earliest and most intense
502 humoral immune response by the host during the early stages of invasion and
503 migration by the parasite (Hanna, 1980a, b; Fairweather et al., 1999), and this also
504 seems to be the case with *F. gigantica* infections in cattle (Hanna and Jura, 1977).
505 While this response has not been shown to engender effective immunoprotection in
506 rats against *F. hepatica* infection (Hanna et al., 1988), the existence of partially
507 protective antigens has been demonstrated by the occurrence of significant
508 resistance to secondary infection with *F. hepatica* in cattle (Doyle, 1971). The
509 evidence for acquisition of acquired immunity to *F. hepatica* infection in experimental
510 hosts and in ruminants has been reviewed by Mulcahy et al. (1999) and Spithill et al.
511 (1999b). Furthermore, Indonesian Thin Tail (ITT) sheep show high resistance
512 against *F. gigantica* infection, which appears to have both innate and acquired
513 features (Roberts et al., 1977a). This may represent an exceptional immunological
514 capacity of ITT sheep to respond to an antigen peculiar to *F. gigantica*, since
515 resistance is not demonstrated against *F. hepatica* (Roberts et al., 1977b; Pleasance
516 et al., 2011a,b). The ability of the invading fluke to continually replace the tegumental
517 glycocalyx apparently enables it to evade the host's innate and acquired immune

responses, by replacing the damaged surface and sloughing off attached host antibody and immune effector cells (Hanna, 1980a; Mulcahy et al., 1999). Insofar as the glycocalyx of larval *F. gigantica* studied here, and that of *F. hepatica* adults examined by Threadgold (1976) may be compared, an important difference is the occurrence of a labile or unattached component (the hyaline layer) in the former. This, although variable in thickness and irregularly preserved, appears to contribute significantly to the overall thickness of the glycocalyx, and may indeed represent the main component of the material sloughed from the surface and replaced by T0 exocytosis, as the larva progresses through the invasion process. The contribution of this mucopolysaccharide (glycosaminoglycan) component of the glycocalyx to the immunological stimulus, as compared to that of the attached glycoprotein/ganglioside layer, is uncertain, but the visualisation of large amounts of flocculent immune complex sloughing from the surface of *F. hepatica* larvae incubated *in vitro* in 10% (v/v) immune sheep serum (Hanna, 1980a) suggests it may be considerable. A comparable ‘immunosloughate’ prepared by incubating live adult *F. hepatica* in a medium containing purified IgG from the sera of *F. gigantica*-infected Indonesian ThinTail sheep was analysed by Cameron et al. (2017), and amongst 38 proteins identified were eight predicted membrane proteins, shared between *F. gigantica* and *F. hepatica,* with potential significance for vaccine development.

4.6 Evolutionary correlates

The unattached, surface-associated mucopolysaccharide layer in invading *F. gigantica* larvae may be analogous to the rhabdite-associated sulphated glycosaminoglycan slime layer in free-living planarians, which has important roles in physical protection, entrapment of extraneous particulate material, and locomotion (McGee et al., 1996; Hayes, 2017).

5. Conclusion

The glycocalyx of the tegumental syncytium in liver flukes is not preserved in its entirety by conventional fixation and preparation techniques for electron microscopy, and requires specific cytochemical methods to enable visualisation. The results of ruthenium red and PATCO staining on *in vitro* penetrated and newly-excysted larvae of *F. gigantica* are consistent with those reported by Threadgold (1976) for adult *F. hepatica*, in that the tegumental glycocalyx shows cytochemical characteristics of a glycoprotein and gangliosidic layer which is carbohydrate–rich and polyanionic throughout its depth, and intimately associated with the outer aspect of the apical plasma membrane. However, in the larvae, an additional thick but irregularly distributed hyaline layer, likely comprising mucopolysaccharide, forms an outermost labile component of the glycocalyx, which usually envelops the underlying dense line and fibrillar layer (Fig. 5). The complex polysaccharides of the parasite surface, together with epithelial cell damage, are likely to evoke the effectors of innate immunity in the naïve host, whilst later in the invasion process, and in immunologically primed hosts, type 1 and type 2 responses of acquired immunity are initiated (Mulcahy et al., 1999). The polyanionic glycocalyx may have a role in absorption and inactivation of cationic effectors such as major basic protein, and may also protect the parasite surface from the action of host- and parasite-derived proteases. The dynamic replacement of damaged tegumental glycocalyx, with attached effectors of host immunity, by exocytosis of T0 secretory bodies at the apical membrane of the syncytium, likely represents the main defence mechanism of early invading *F. gigantica* larvae at the interface with the host.

Conflict of interest

No actual or potential conflict of interest was identified that could inappropriately influence or be perceived to influence, the outcome of this work.

Acknowledgements

Our thanks are due to Mr R. Ogola and Ms E. Wairimu of the Department of Parasitology, East African Veterinary Research Organisation, Muguga, Kenya, for expert technical assistance. Thanks are also due to Ms N. Dobson (Librarian, QUB / AFBI) and Mr C. Mason (Photographer, AFBI) for assistance and advice. No external funding was obtained for this work. M.W.R. was supported by grants (BB/L019612/1 and BB/N017757/1) from the Biotechnology and Biological Sciences Research Council (BBSRC).

References

Ahmad, M., Nizami, W.A., Hanna, R.E.B., 1988. Topographical studies of two digenetic trematodes of buffalo by scanning electron microscopy. Zool. Anz. 220, 59-64.

Allen, J.E., Maizels, R.M., 2011. Diversity and dialogue in immunity to helminths. Nat. Rev. Immunol. 11, 375–388.

Andrews, S.J., 1999. The life cycle of *Fasciola hepatica*. In: Dalton, J.P. (Ed.), Fasciolosis. CAB Publishing International, Oxon, pp. 1–29.

Bennett, C.E., 1975. *Fasciola hepatica*: development of caecal epithelium during migration in the mouse. Exp. Parasitol. 37, 426-441.

591 Bennett, C.E., Threadgold, L.T., 1975. *Fasciola hepatica*: development of tegument
592 during migration in mouse. Exp. Parasitol. 38, 38-55.

593 Cameron, T.C., Cooke, I., Faou, P., Toet, H., Piedrafita, D., Young, N.,
594 Rathinasamy, V., Beddoe, T., Anderson, G., Dempster, R., Spithill, T.W., 2017. A
595 novel *ex vivo* immunoproteomic approach characterising *Fasciola hepatica*
596 tegumental antigens identified using immune antibody from resistant sheep. Int. J.
597 Parasitol. 47, 555-567.
598 Cwiklinski, K., Donnelly, S., Drysdale, O., Jewhurst, H., Smith, D., De Marco
599 Verissimo, C., Pritsch, I.C., O'Neill, S., Dalton, J.P. & Robinson, M.W., 2019. The
600 cathepsin-like cysteine peptidases of trematodes of the genus *Fasciola*. Adv.
601 Parasitol. 104, 113-164.

602 Dalton, J.P., Robinson, M.W., Mulcahy, G., O'Neill, S.M., Donnelly, S., 2013.
603 Immunomodulatory molecules of *Fasciola hepatica*: candidates for both vaccine and
604 immunotherapeutic development. Vet. Parasitol. 195, 272-285.

605 Dangprasert, T., Khawsuk, W., Meepool, A., Wanichanon, C., Viyanant, V.,
606 Upatham, E.S., Wongratanacheevin, S., Sobhon, P., 2001. *Fasciola gigantica*:
607 surface topography of the adult tegument. J. Helminthol. 75, 43-50.
608 de la Torre-Escudero, E., Manzano-Román, R., Valero, L., Oleaga, A., Pérez-
609 Sánchez, R., Hernández-González, A., Siles-Lucas, M., 2011.Comparative
610 proteomic analysis of *Fasciola hepatica* juveniles and *Schistosoma bovis*
611 schistosomula. J. Proteomics 74 (9), 1534–1544.
612 de la Torre Escudero, E., Gerlach, J.Q., Bennett, A.P.S., Cwiklinski, K., Jewhurst,
613 H.L., Huson, K.M., Joshi, L., Kilcoyne, M., O'Neill, S.M., Dalton, J.P., Robinson,
614 M.W., 2019. Surface molecules of extracellular vesicles secreted by the helminth

615 pathogen *Fasciola hepatica* direct their internalisation by host cells. PLoS Negl.
616 Trop. Dis. 13(1):e0007087.

617 Dixon, K.E., 1964. Excystment of metacercariae of *Fasciola hepatica* L. *in vitro*.
618 Nature 202, 1240-1241.

619 Doyle, J.J., 1971. Acquired immunity to experimental infection with *Fasciola*
620 *hepatica* in cattle. Res. Vet. Sci.12, 527-534.

621 Fairweather, I., Threadgold, L.T., Hanna, R.E.B., 1999. Development of *Fasciola*
622 *hepatica* in the mammalian host. In: Dalton, J.P. (Ed.), Fasciolosis. CAB Publishing
623 International, Oxon, pp. 47–111.

624 Hanna, R.E.B., 1980a. *Fasciola hepatica*: glycocalyx replacement in the juvenile as
625 a possible mechanism for protection against host immunity. Exp. Parasitol. 50,
626 103-114.

627 Hanna, R.E.B., 1980b. *Fasciola hepatica*: an immunofluorescent study of antigenic
628 changes in the tegument during development in the rat and the sheep. Exp.
629 Parasitol. 50, 155-170.

630 Hanna, R.E.B., Anderson, A., Trudgett, A.G., 1988. *Fasciola hepatica*: studies on
631 vaccination of rats and mice with a surface antigen prepared from fluke homogenate
632 by means of a monoclonal antibody. Res. Vet. Sci. 44, 237-241.

633 Hanna, R.E.B., Jura, W., 1977. Antibody response of calves to a single infection of
634 *Fasciola gigantica* determined by an indirect fluorescent antibody technique. Res.
635 Vet. Sci. 22, 339-342.

636 Hanna, R.E.B., Moffett, D., Robinson, M.W., Jura, W.G.Z.O., Brennan, G.P.,
637 Fairweather, I., 2019. *Fasciola gigantica*: comparison of the tegumental ultrastructure
638 in newly-excysted metacercariae and *in vitro* penetrated juvenile flukes indicates

639 intracellular sources of molecules with vaccinal and immunomodulatory potential.
640 Vet. Parasitol. 265, 38-47.

641 Hayat, M.A., 1989. Principles and Techniques of Electron Microscopy, Biological
642 Applications, third edition. The Macmillan Press Ltd., Hampshire, UK, pp. 208-326
643 (Chapter 4).

644 Hayes, M.J., 2017. Sulphated glycosaminoglycans support an assortment of
645 planarian rhabdite structures. Biology Open 6, 571-581; doi: 10.1242/bio.024554.

646 Jackson, J.A., Friberg, I.M., Little, S., Bradley, J.E., 2009. Review series on
647 helminths, immune modulation and the hygiene hypothesis: immunity against
648 helminths and immunological phenomena in modern human populations:
649 coevolutionary legacies? Immunology 126,18–27.

650 Kumar, V., Abbas, A.K., Aster, J.C., 2018. Robbins Basic Pathology, tenth edition.
651 Elsevier, Philadelphia, Pennsylvania, USA, pp. 57-96 (Chapter 3).

652 McGee, C., Fairweather, I., Blackshaw, R.P., 1996. Ultrastructural observations on
653 rhabdite formation in the planarian, *Artioposthia triangulata*. J. Zool. (Lond.) 240,
654 563-572.

655 McVeigh, P., Cwiklinski, K., Garcia-Campos, A., Mulcahy, G., O'Neill, S.M., Maule,
656 A.G., Dalton, J.P., 2018. *In silico* analyses of protein glycosylating genes in the
657 helminth *Fasciola hepatica* (liver fluke) predict protein-linked glycan simplicity and
658 reveal temporally dynamic expression profiles. Sci.Rep. 8, 1170;
659 doi:10.1038/s41598-018-29673-3.

660 Mulcahy, G., Joyce, P., Dalton, J.P., 1999. Immunology of *Fasciola hepatica*
661 infection. In: Dalton, J.P. (Ed.), Fasciolosis. CAB Publishing International, Oxon, pp.
662 341–375.

663 Pearse, A.G.E., 1985. Histochemistry Theoretical and Applied, fourth edition.
664 Churchill Livingstone, New York, USA, pp. 675-753 (Chapter 15).

665 Piedrafita, D., Spithill, T.W., Smith, R.E., Raadsma, H.W., 2010. Improving animal
666 and human health through understanding liver fluke immunology. Parasite
667 Immunol. 32, 572-81.
668 Pleasance, J., Raadsma, H.W., Estuningsih, S.E., Widjajanti, S., Meeusen, E.,
669 Piedrafita, D., 2011a. Innate and adaptive resistance of Indonesian Thin Tail sheep
670 to liver fluke: a comparative analysis of *Fasciola gigantica* and *Fasciola hepatica*
671 infection. Vet. Parasitol. 178, 264-72.
672 Pleasance, J., Wiedosari, E., Raadsma, H.W., Meeusen, E., Piedrafita, D., 2011b.
673 Resistance to liver fluke infection in the natural sheep host is correlated with a
674 type-1 cytokine response. Parasite Immunol. 33, 495-505.
675 Rambourg, A., 1971. Morphological and histochemical aspects of glycoproteins at
676 the surface of animal cells. Int. Rev. Cytol. 31, 57-114.

677 Ravidà, A., Cwiklinski, K., Aldridge, A.M., Clarke, P., Thompson, R., Gerlach, J.Q.,
678 Kilcoyne, M., Hokke, C.H., Dalton, J.P., O'Neill, S.M., 2016. *Fasciola hepatica*
679 surface tegument: glycoproteins at the interface of parasite and host.
680 Mol. Cell Proteomics 15, 3139-3153.

681 Roberts, J.A., Estuningsih, E., Widjayanti, S., Wiedosari, E., Partoutomo, S., Spithill,
682 T.W., 1997a. Resistance of Indonesian thin tail sheep against *Fasciola gigantica* and
683 *F. hepatica*. Vet. Parasitol. 68, 69-78.

684 Roberts, J.A., Estuningsih, E., Wiedosari, E., Spithill, T.W., 1997b. Acquisition of
685 resistance against *Fasciola gigantica* by Indonesian thin tail sheep. Vet. Parasitol.
686 73, 215-24.
687 Rogan, M.T., Threadgold, L.T., 1984. *Fasciola hepatica*: tegumental alterations as a
688 consequence of lectin binding. Exp. Parasitol. 57, 248-260.

689 Sobhon, P., Anantavara, S., Dangprasert, T., Viyanant, V., Krailas, D., Upatham,
690 E.S., Wanichanon, C., Kusamran, T., 1998. *Fasciola gigantica*: studies of the
691 tegument as a basis for the developments of immunodiagnosis and vaccine.
692 Southeast Asian J. Trop. Med. Public Health 29, 387-400.
693 Spithill, T.W., Smooker, P.M., Copeman, D.B., 1999a. *Fasciola gigantica*:
694 epidemiology, control, immunology and molecular biology. In: Dalton, J.P. (Ed.),
695 Fasciolosis. CAB Publishing International, Oxon, pp. 465-–525.

696 Spithill, T.W., Smooker, P.M., Sexton, J.L., Bozas, E., Morrison, C.A., Creaney, J.,
697 Parsons, J.C., 1999b. Development of vaccines against *Fasciola hepatica*. In:
698 Dalton, J.P. (Ed.), Fasciolosis. CAB Publishing International, Oxon, pp. 377-–410.

699 Suvarna, S.K., Layton, C., Bancroft, J.B., 2019. Bancroft's Theory and Practice of
700 Histological Techniques, eighth edition. Elsevier Limited, pp. 176-197 (Chapter 13).

701 Threadgold, L.T., 1976. *Fasciola hepatica*: ultrastructure and histochemistry of the
702 glycocalyx of the tegument. Exp. Parasitol. 39, 119-134.

703 Threadgold, L.T., Brennan, G., 1978. *Fasciola hepatica*: basal infolds and associated
704 vacuoles of the tegument. Exp. Parasitol. 46, 300-316.

705 Varki, A., Schauer, R., 2009. Sialic Acids. In**:** Varki**,** A., Cummings, R.D., Esko,
706 J.D., Freeze, H.H., Stanley, P., Bertozzi, C.R., Hart, G.W., Etzler, M.E., (Eds.),

Essentials of Glycobiology, second edition. Cold Spring Harbor Laboratory Press (Chapter 14).

Table 1

Summary of staining methods and controls.

Staining method	Control	Purpose
Ruthenium red-glutaraldehyde-cacodylate buffer		Fix and stain anion-rich macromolecules, viz. glycoproteins, glycolipids, mucopolysaccharides
	(1) Omit ruthenium red: glutaraldehyde-cacodylate fixation only	No selective fixation or staining of anion-rich macromolecules: conventional fixation and staining
	(2) Neuraminidase	Cleaves sialic acid: partial breakdown of glycoproteins, glycolipids, (mucopolysaccharides ?[3])
PATCO[1]-paraformaldehyde-Millonig buffer		Fix and stain aldehydes generated by PA[2] in glycoproteins, glycolipids, mucopolysaccharides
	(1) Omit PA[2] treatment	Only pre-existing or fixative-introduced aldehydes fixed and stained
	(2) Aniline or dimedone before PA[2] treatment	Blocks pre-existing or fixative-introduced aldehydes
	(3) Aniline or dimedone after PA[2] treatment	Blocks aldehydes generated by PA[2]
	(4) Neuraminidase	Cleaves sialic acid: partial breakdown of glycoproteins, glycolipids, (mucopolysaccharides ?[3])

[1] PATCO = Periodic acid-thiocarbohydrazine-osmium

[2] PA = Periodic acid

[3] (mucopolysaccharides?) = Mucopolysaccharides in *Fasciola* have not been shown to contain sialic acid but are lost with neuraminidase treatment, possibly due to destabilisation of the underlying glycoproteins and glycolipids, or non-specific removal by the additional procedural steps.

Figure Captions

Fig. 1. (a–e) Electron micrographs of *Fasciola gigantica*, penetrated larvae, treated *en bloc* with ruthenium red, but sections left without further staining. (a) A continuous line of dense staining (dl) is present on the outer aspect of the apical membrane, immediately beneath which the electron-lucid core and dense inner lamina of the membrane are visible (black arrows). Superficially, there is a sparse dense fibrillar layer (fl). In the cytoplasm of the tegumental syncytium, secretory bodies (T0) are evident, many having a flattened or rod-like profile, and large tertiary lysosomes (so-called 'dense bodies', db) are present. **Inset** shows the surface between X and Y enlarged to emphasise the electron-lucid core (arrowed) and the continuous dense line (dl) apposed to the intermittent strands of the fibrillar layer (fl). (b) In many areas, the dense line (dl) and fibrillar layer (fl), which closely follow the invaginations of the surface, are covered with moderately-stained, relatively featureless hyaline material (hm), beneath which the staining of the former features is less pronounced (white arrow). Secretory bodies (T0) with elliptical or flattened profiles are evident in the syncytial cytoplasm and, in places, the electron-lucid core and dense inner lamina of the apical membrane are visible (black arrow). (c) The hyaline material (hm) forms an irregular and discontinuous, sometimes globular layer, enveloping the dense line (dl) and fibrillar layer (fl), which are often less densely stained beneath it (white arrows). The hyaline material sometimes incorporates electron-dense patches and filaments resembling components of the fibrillar layer (black arrows). T0 = tegumental secretory body. (d) The hyaline material (hm) is seen apparently elevating the dense line (dl) and fibrillar layer (fl). T0 = tegumental secretory body. (e) In some areas the ruthenium red-stained complex, including hyaline material (hm) and dense line (dl) with fibrillar layer, sloughs from

769 the surface as membranous strips, whorls and vesicles (arrows). T0 = flattened
770 profile of tegumental secretory body.

771 **Fig. 2**. Electron micrographs of *Fasciola gigantica* , newly-excysted larvae (a, d) and
772 penetrated larvae (b, c, e); treated *en bloc* with ruthenium red, but sections left
773 without further staining (a-c, e) or untreated with ruthenium red but sections stained
774 with uranyl acetate and lead citrate (d). (a) A dense line (dl) and fibrillar layer (fl) are
775 closely applied to the outer aspect of the apical plasma membrane of the tegumental
776 syncytium, following its invaginations and valleys that have open contact with the
777 surface (arrows). In some areas, an irregular outermost layer of hyaline material
778 (hm) envelops the surface. TS = cytoplasm of the tegumental syncytium, unstained
779 by ruthenium red. (b) The tegumental secretory bodies (T0) in the surface syncytium
780 are not stained by ruthenium red, but are sometimes seen discharging their content
781 at the surface (black arrow) apparently contributing to the hyaline material (hm), and
782 becoming flattened in the process. dl = dense line; fl = fibrillar layer. (c) Tegumental
783 secretory bodies (T0) approach the apical plasma membrane to contribute their
784 content (black arrow) to the hyaline material (hm), becoming flattened in the process.
785 Elsewhere on the surface, the dense line (dl) and fibrillar layer (fl) of the glycocalyx
786 are clearly evident. (d) The tegumental surface of a conventionally-fixed larva,
787 stained with uranyl acetate and lead citrate, shows a thin, poorly-defined ‘fuzzy’
788 glycocalyx on the outer aspect of the apical membrane (black arrows). The full
789 thickness of the glycocalyx has not been preserved. The electron-lucid core of the
790 apical membrane (white arrow) is visible beneath. A flattened tegumental secretory
791 body (T0) is present in the cytoplasm. (e) Treatment with neuraminidase before
792 ruthenium red *en bloc* staining. On the apical plasma membrane, the dense line and
793 fibrillar layer of the glycocalyx (arrowed) are less well-defined than in the test

sections. Hyaline material is missing in this section. T0 = flattened tegumental secretory body.

Fig. 3. Electron micrographs of *Fasciola gigantica* larvae, penetrated (a-d) and newly-excysted (e), stained *en bloc* using the periodic acid-thiocarbohydrazine-osmium (PATCO) technique. (a) The surface of the apical plasma membrane of the tegumental syncytium bears a zone of dense staining (dz), approximately 100nm thick, but varying considerably throughout the body. This follows closely the contours of the surface (arrow), albeit appearing cracked. Tegumental secretory bodies (T0) in the syncytial cytoplasm are stained, especially those closer to the surface, and there is some patchy staining over the cytoplasm itself (TS). (b) The dense zone (dz) tends to crack and break, often cleaving from the surface at the level of the apical plasma membrane (arrows). T0 = tegumental secretory bodies in the syncytial cytoplasm. (c) The dense zone (dz), representing the full depth of the glycocalyx, is fragmented and partially detached from the underlying tegumental syncytium (TS). The latter contains secretory bodies (T0) which are moderately stained by the PATCO technique, and 'dense bodies' (db), representing heterophagosomes, which are unstained. (d) A moderately stained secretory body (T0) in the tegumental syncytium lies immediately beneath the apical surface, apparently contributing its contents (arrow) to the dense zone (dz), which represents the glycocalyx. Heterophagosomes (db) in the syncytium, are unstained. (e) A thick but irregular densely-stained zone (dz), representing the glycocalyx, is present over the apical surface of the tegument. In the underlying syncytium (TS), moderately-stained secretory bodies (T0) are present.

Fig. 4. Electron micrographs of *Fasciola gigantica* larvae, penetrated (a, b, d) and newly-excysted (c), *en bloc* controls for the PATCO technique. (a) Periodic acid

treatment omitted. The apical plasma membrane of the tegumental syncytium is lightly delineated (arrow), and there is a fine speckling of non-specific osmium dioxide deposition over the syncytial cytoplasm (TS), but there is no positive PATCO staining. (b) Treated with dimedone after periodic acid treatment but before thiocarbohydrazine-osmium (TCH) treatment. Staining of the glycocalyx is reduced to irregularly distributed dense particles on the apical plasma membrane (arrow), and there is patchy staining over the syncytial cytoplasm (TS). (c) Treated with aniline after periodic acid treatment but before TCH treatment. The apical plasma membrane is delineated by light irregular dense particulate staining (arrow). Secretory bodies (T0) in the syncytium are moderately stained. (d) Neuraminidase treatment before PATCO staining. Glycocalyx staining is reduced to irregularly-distributed dense patches on the apical membrane (black arrows). There is patchy non-specific staining over the syncytial cytoplasm (TS) that corresponds to non-membrane-bound polymorphic masses of mucopolysaccharide (white arrows).

Fig. 5.

Diagram of the apical plasma membrane of the tegumental syncytium of *Fasciola gigantica* (based on that for *Fasciola hepatica* shown by Threadgold, 1976). This illustrates the relationship between the proposed molecular structure of the gylcocalyx and the respective layers of the fixed and labile components as demonstrated by ruthenium red and PATCO staining (viz. dense line, fibrillar layer and hyaline layer). The labile mucopolysaccharide hyaline layer is envisaged as incomplete and irregular, prone to partial removal during preparative procedures.

843 **Figure 1**

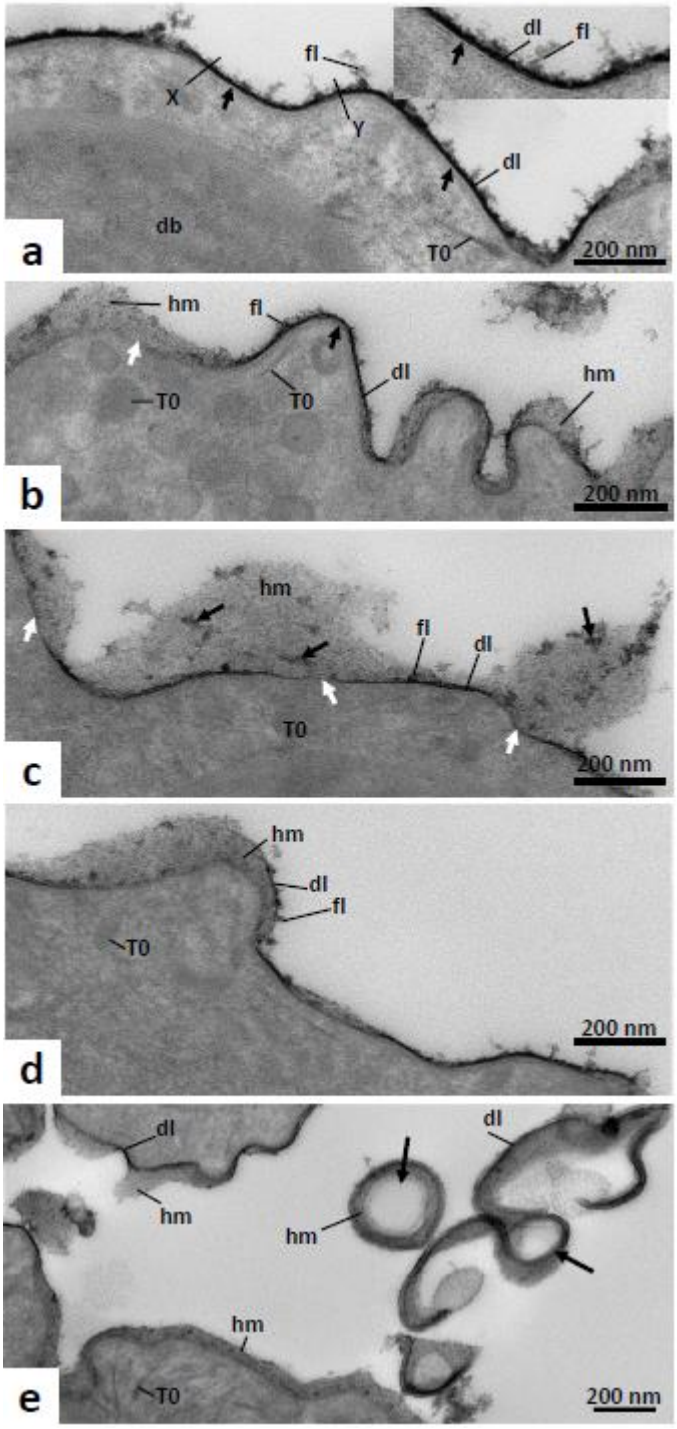

844

845

846 **Figure 2**

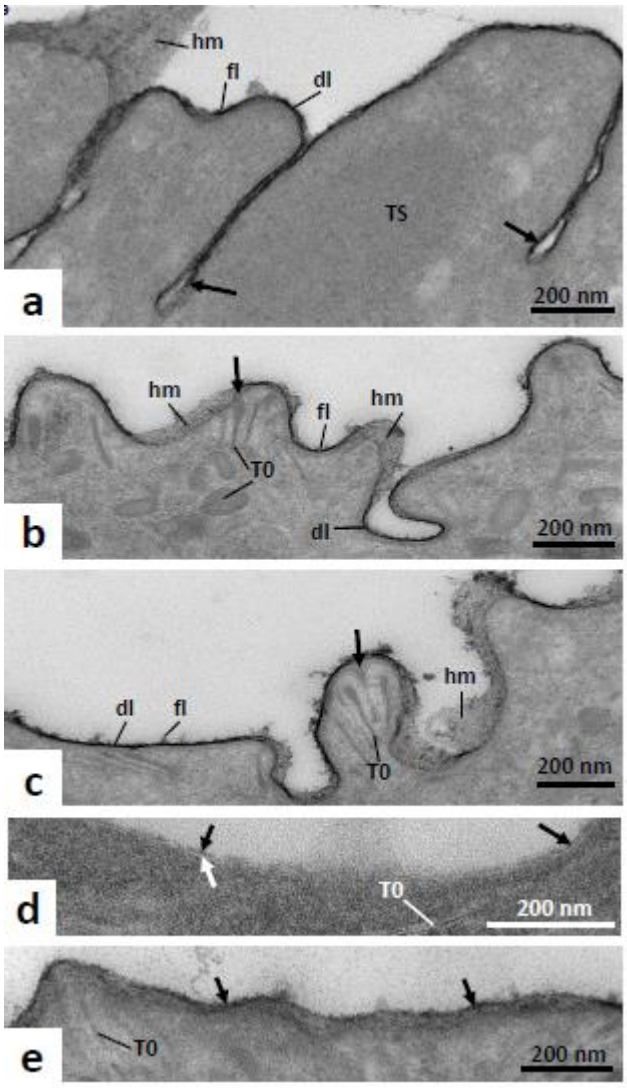

847

848 **Figure 3**

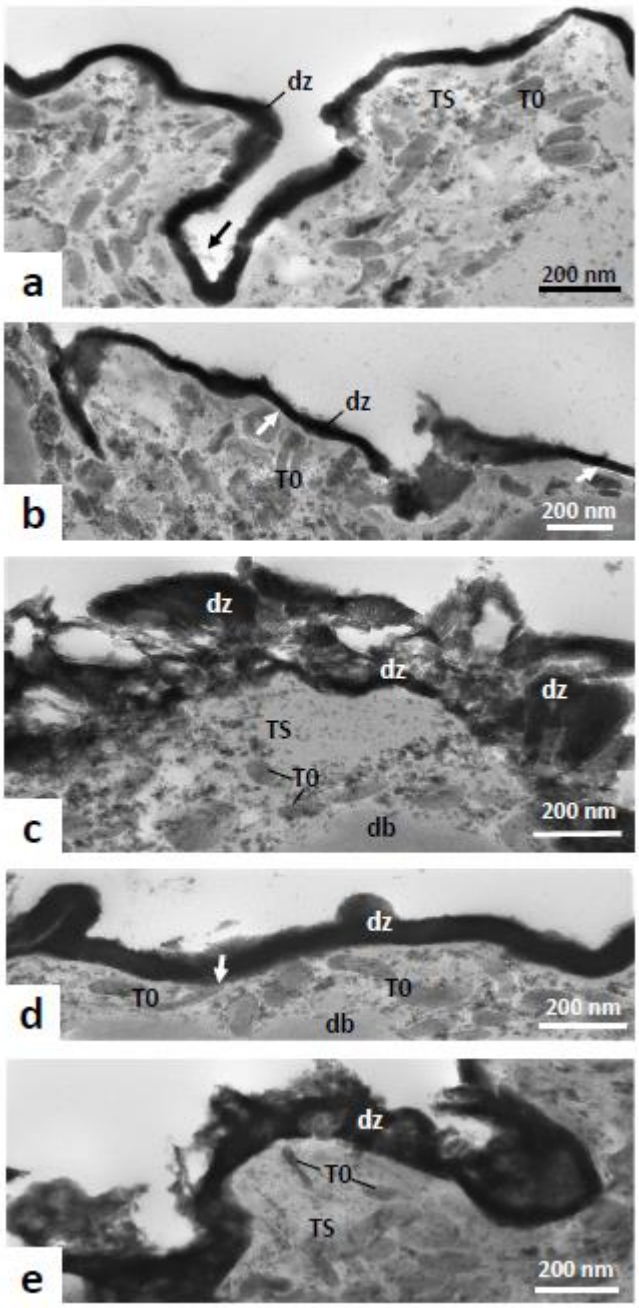

849

850 **Figure 4**

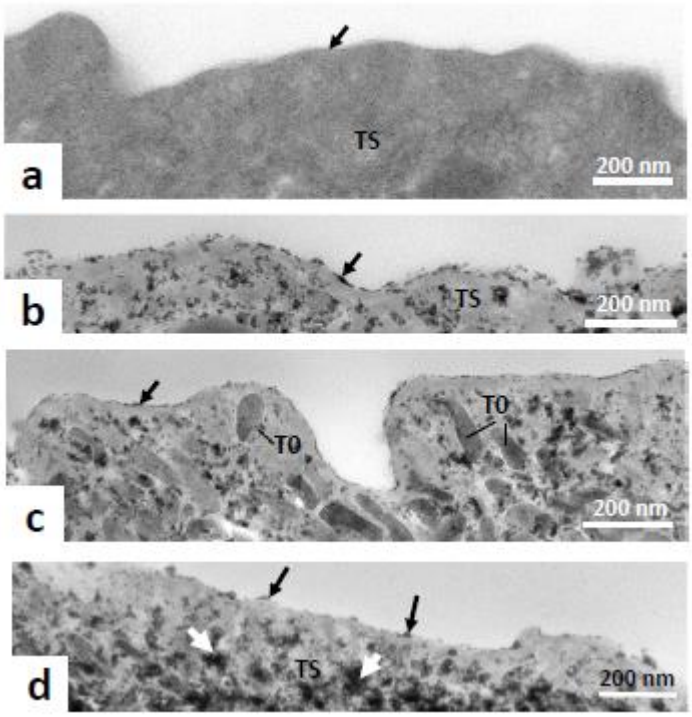

851

852 **Figure 5**

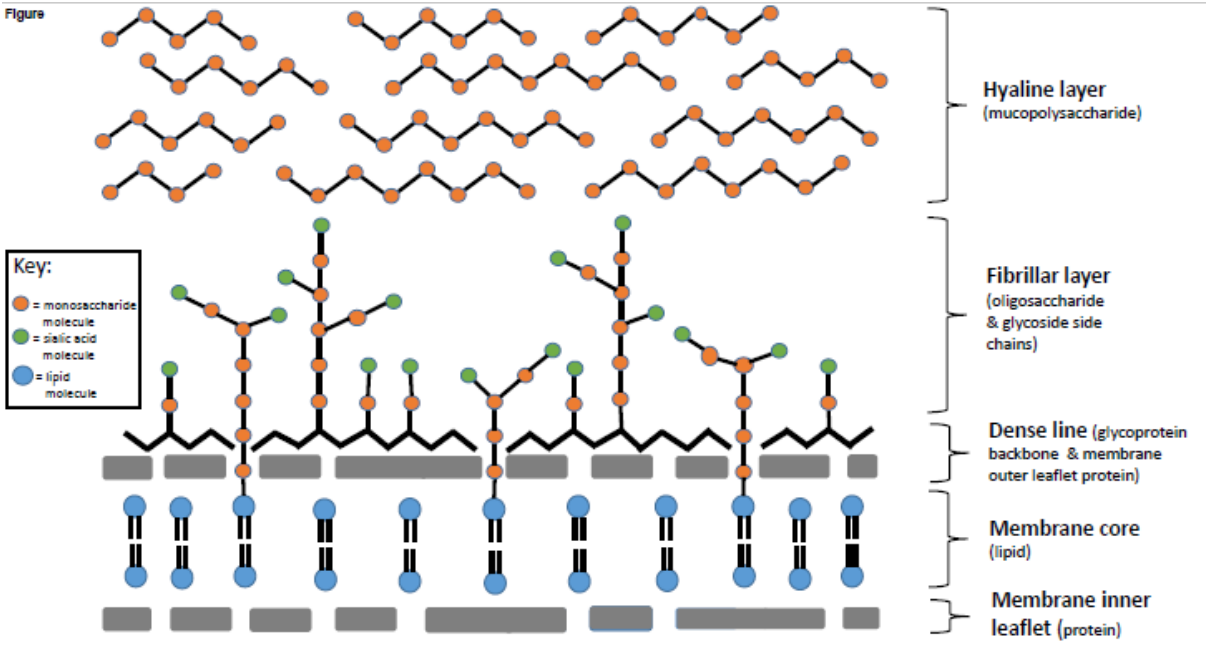

853